J. theor. Biol. (2003) **220,** 285–301
doi:10.1006/jtbi.2003.3136, available online at http://www.idealibrary.com on IDEAL®

Heterogeneous Perfusion is a Consequence of Uniform Shear Stress in Optimized Arterial Tree Models

Wolfgang Schreiner*†, Rudolf Karch†, Martin Neumann‡, Friederike Neumann†, Susanne M. Roedler§ and Georg Heinze†

†*Department of Medical Computer Sciences, University of Vienna, Department of Medical Computer Sciences Spitalgasse* 23, *A*-1090 *Vienna, Austria* ‡*Institute of Experimental Physics, University of Vienna, Department of Medical Computer Sciences Spitalgasse* 23, *A*-1090 *Vienna, Austria and* §*Department of Cardiology, University of Vienna, Department of Medical Computer Sciences Spitalgasse* 23, *A*-1090 *Vienna, Austria*

(*Received on* 26 *March* 2002, *Accepted in revised form on* 22 *July* 2002)

Using optimized computer models of arterial trees we demonstrate that flow heterogeneity is a necessary consequence of a uniform shear stress distribution. Model trees are generated and optimized under different modes of boundary conditions. In one mode flow is delivered to the tissue as homogeneously as possible. Although this primary goal can be achieved, resulting shear stresses between blood and the vessel walls show very large spread. In a second mode, models are optimized under the condition of uniform shear stress in all segments which in turn renders flow distribution heterogeneous. Both homogeneous perfusion and uniform shear stress are desirable goals in real arterial trees but each of these goals can only be approached at the expense of the other. While the present paper refers only to optimized models, we assume that this dual relation between the heterogeneities in flow and shear stress may represent a more general principle of vascular systems.

Introduction

In principle, arterial trees serve the purpose of supplying all parts of tissue with blood at physiologically necessary values of pressures and flows. This functionality is of vital importance and costly in terms of energy: mechanical energy is needed to maintain flow and chemical energy is needed to maintain the total volume of blood in a functioning condition. Due to these reasons it is widely assumed that the arterial system has undergone certain optimization processes during phylogeny (LaBarbera, 1990; Zamir & Bigelow, 1984; Murray & Oster, 1984; Lefevre, 1982, 1983; Uylings, 1977; Kamiya *et al.*, 1974; Kamiya & Togawa, 1972; Rosen, 1967; Cohn, 1954; Thompson, 1942; Murray, 1926a). In particular, theoretical arguments suggest that the overall expenditure of energy can be minimized if the total volume of blood (i.e. the "intravascular" volume, V_{tot}) is minimized and simultaneously the radii of arterial segments at bifurcations follow a "power" law (Kurz *et al.*, 1997; van Bavel & Spaan, 1992; Zamir *et al.*, 1992; Zamir, 1988a; Sherman, 1981)

$$r_0^\gamma = r_1^\gamma + r_2^\gamma \tag{1}$$

* Corresponding author. Tel.: +43-1-40400-6679; fax: +43-1-40400-6677
E-mail address: wolfgang.schreiner@akh-wien.ac.at (W. Schreiner).

0022-5193/03/$35.00

with r_0, r_1 and r_2 being the radii of the parent segment, the larger and the smaller daughter ($r_1 \geqslant r_2$). For stationary (non-pulsatile) flow the bifurcation exponent $\gamma = 3$ is considered optimum, whereas pulsatile flow finds optimum conductance around $\gamma = 2.55$ (Arts *et al.*, 1979). Although real arterial trees fulfill eqn (1) only in a statistical rather than in a precise mathematical sense, the formula represents the most suitable choice in the frame of optimization models and will be adopted in the present work with $\gamma = 3$. Similarly, even though quantities other than the intravascular volume may have influenced phylogenetic optimization and can be evaluated in models (Schreiner *et al.*, 1995), the minimization of V_{tot} has become a golden standard in modeling (Sherman, 1981; Zamir, 1976; Kamiya *et al.*, 1974; Kamiya & Togawa, 1972) and will be adopted in the present work.

Volume minimization and a bifurcation law [eqn (1)] lend themselves as a nucleus of principles for constructing arterial tree models on the computer. In the present work the models consist of binary branching cylindrical tubes. These are perfused under physiologically reasonable (boundary) conditions of pressures and flows, derived from a generalized formulation for the "task of supply" as follows.

Boundary Conditions for Pressures

The task of blood delivery through arterial trees ends at the pre-capillary level where a characteristic (pre-capillary) pressure is required to enable transcapillary metabolic exchange (Kamiya & Togawa, 1972). Hence we require for the model that a unique pressure (p_{term}) should prevail at all terminal outlets. Assuming a given perfusion pressure (p_{perf}) at the entrance of the feeding arterial segment, the model carries the total perfusion flow (Q_{perf}) across a pressure difference $\Delta p = p_{\text{perf}} - p_{\text{term}}$. Each segment i (length l_i, pressure gradient Δp_i across segment, blood viscosity η) is perfused according to Poiseuille's law (Fung, 1997)

$$Q_i = \frac{\pi}{8\eta}\frac{r_i^4}{l_i}\Delta p_i. \tag{2}$$

The magnitude of p_{term} is not directly preset but rather adapted to permit a given total flow (Q_{perf}) for given p_{perf} and a given radius of the root segment (Karch *et al.*, 2000a). The latter can be taken from morphometric measurements on representative arterial beds (Kassab *et al.*, 1993).

Boundary Conditions Related to Flow

The total flow Q_{perf} through the feeding artery may be distributed over the dependent (distal) arterial bed (of the model) according to several alternative principles, formulated as *boundary conditions*. Two such modes will be considered in the present work.

PRESCRIBING TERMINAL PRESSURES AND FLOWS AS BOUNDARY CONDITIONS (MODE PTP-F)

This mode makes the model reproduce any given (and arbitrarily) prescribed terminal flow distribution. For example, the goal may be a distribution as even as possible, yielding (almost) equal perfusion densities in all microcirculatory regions (Karch *et al.*, 1999; Schreiner & Buxbaum, 1993). Alternatively, a gradient in perfusion density may be prescribed across an organ, as for example would be appropriate between the epicardial and endocardial layers of the ventricular wall of the heart (Brown & Egginton, 1988; Schubothe *et al.*, 1983; Karch *et al.*, 2000a). In any of these cases the flow through each of the N_{term} terminal segments is prescribed as a boundary condition. Due to conservation of mass, flows in all (N_{term}–1) non-terminal, bifurcating segments result from simple additions:

$$Q_0 = Q_1 + Q_2. \tag{3}$$

Boundary conditions of type PTP-F allow one to compute the radii of all $2N_{\text{term}}$–1 segments with given locations (coordinates) and connective structure (Schreiner *et al.*, 1996; Schreiner & Buxbaum, 1993; Pries *et al.*, 1990). A corresponding value for the total intravascular volume (V_{tot}) is obtained from

$$V_{\text{tot}}/\pi = \sum_{i=1}^{N_{\text{tot}}} l_i^{\mu} r_i^{\lambda} \quad \text{with} \quad \mu = 1,\ \lambda = 2. \tag{4}$$

PRESCRIBING TERMINAL PRESSURES AND UNIFORM SHEAR STRESS AS BOUNDARY CONDITIONS (MODE PTP-USS)

In this mode terminal flows are not prescribed but rather computed so as to let the shear stress

$$\tau_i = \frac{4\eta Q_i}{\pi r_i^3} = \eta\,\dot{\gamma}_i \tag{5}$$

between blood and the arterial wall be uniform in all segments i over the entire tree.* This makes sense, since shear stress is considered a crucial parameter of vascular regulatory mechanisms (Hazel & Pedley, 2000; Skalak & Price, 1996; Hacking *et al.*, 1996; Pries *et al.*, 1995; Girard & Nerem, 1995; Jones *et al.*, 1993; Davies *et al.*, 1984; Franke *et al.*, 1984; Gimbrone-MA, 1999) and pathophysiology (Yung & Frojmovic, 1982; Hellums & Hardwick, 1981; Rodbard, 1975; Leverett *et al.*, 1972). Excessive values of shear stress, both very small and very large ones, are deemed harmful in causing either aggregation due to stagnation zones or thrombosis due to the activation of thrombocytes (Caro *et al.*, 1995; Topper & Gimbrone-MA, 1999; Hellums & Hardwick, 1981). A so-to-speak "optimum" situation, with a totally uniform shear stress throughout the tree, can be realized in the computer model by adopting boundary conditions as follows: (i) The bifurcation exponent is set to $\gamma = 3$ and (ii) the flow ratio between sister terminals i and j (having the same parent) is set to yield equal shear stresses and equal pressure drops (for the given lengths l_i and l_j resulting from segment coordinates):

$$Q_i/r_i^3 = Q_j/r_j^3 \quad \text{and} \quad (Q_i l_i)/r_i^4 = (Q_j l_j)/r_j^4. \tag{6}$$

Due to eqn (6) the ratio of flows in sister terminals is given by

$$Q_j/Q_i = (l_j/l_i)^3. \tag{7}$$

If any sisters (terminal as well as bifurcating) experience equal shear stresses, their parent's shear stress will assume the very same value, provided $\gamma = 3$, as can be shown by combining eqns (1), (3) and (5). The general case, where the flows into two subtrees have to be balanced under uniform shear stress conditions can be tackled by the concept of equivalent ducts or 'reduced' resistances (Karch *et al.*, 1999): each subtree is replaced by an "equivalent segment" whose length l_j^* is chosen to yield the same resistance (R_j) as the subtree for the same entrance radius (r_j),

$$\frac{8\eta}{\pi}\frac{l_j^*}{r_j^4} = R_j. \tag{8}$$

This is always possible for equal terminal pressures (Zhou *et al.*, 1999), regardless of the connective structure and geometry of the model tree. In summary, by choosing terminal flows according to eqns (7) and (8) at a bifurcation exponent of $\gamma = 3$ it is possible to implement constant shear stress throughout the entire model tree.

In the present work we evaluate the consequences for structure and hemodynamic functionality induced by the two types of boundary conditions, uniform flow (PTP-F) vs. uniform shear stress (PTP-USS).

Materials and Methods

CONSTRAINED CONSTRUCTIVE OPTIMIZATION (CCO)

The method of CCO has been described in detail previously (Schreiner & Buxbaum, 1993; Schreiner, 1993) and draws on an iterative process similar to induction: *given* a binary tree of straight cylindrical tubes, constraints are implemented as outlined above, and we describe how to grow the tree by another bifurcation (i.e. two new segments). To these ends the following items have to be specified: (i) the process of construction and (ii) a concept for optimization.

Process of Construction

A perfusion domain is defined mathematically, representing the (part of the) organ to be perfused. Within this domain the model is constructed by adding one segment after the

* In the scientific literature the symbol γ (dimensionless) is widely used for the bifurcation exponent and $\gamma(s^{-1})$ is used for the shear rate. In order to keep notation compatible we stick to these conventions and hope not to cause confusion. In the present context γ is a constant and $\dot{\gamma}$ *is not* its time derivative.

other as follows: a new site of perfusion is drawn from a "random sequence" (Knuth, 1973) and is checked for not being too close to any of the existing segments or terminal sites (Karch *et al.*, 1999; Schreiner & Buxbaum, 1993), otherwise tossing is repeated. The new terminal is connected to a segment (i_{conn}) of the existing tree and constraints are implemented, making the grown tree fulfill the very same boundary conditions as its predecessor. Both procedures, selecting the segment i_{conn} and choosing the geometrical location of the new bifurcation, are subjected to optimization as described below.

Random sequences may be started from different seeds (Knuth, 1973), yielding different samples of terminal sites with the same type of spatial distribution.

Concepts for Optimization

Given a bifurcation (e.g. segment i_{bif}) located at coordinates $\mathbf{x}_{bif}$ within an existing model, a specific value of V_{tot} is obtained after implementing the constraints (see above). Moving the bifurcation ($\mathbf{x}_{bif} \rightarrow \mathbf{x}_{bif} + \delta\mathbf{x}$), in general changes the lengths of the three adjacent segments, yielding a different value of $V_{tot} \rightarrow V_{tot} + \delta V$ upon re-implementation of the constraints. This offers the possibility to displace the bifurcation not arbitrarily but rather along the gradient (Fröberg, 1985) toward the minimum (i.e. optimum) of V_{tot} (geometrical optimization). Once the proper segment i_{conn} for the connection is found, the new bifurcation can be geometrically optimized by this procedure.

In order to find the proper segment i_{conn}, each segment in the vicinity of the new terminal is tentatively used as connection site, the bifurcation is geometrically optimized, the specific value of V_{tot} is recorded, and the connection dissolved again. Finally that segment which yields the lowest V_{tot} is accepted as the permanent connection site. Note that geometric optimization is nested within this structural optimization.

The described method of model generation is based on the repetitive implementation of constraints during a stepwise construction and optimization process [constrained constructive optimization, (CCO), Schreiner, 1993; Schreiner & Buxbaum, 1993]. Connective structure as well as geometry of the tree, including radii and branching angles, result from boundary conditions and optimization principles rather than being plugged in. Each step of development influences all following steps.

Results

MODEL TREES WITH HOMOGENEOUS PERFUSION VS. MODELS WITH UNIFORM SHEAR STRESS

The CCO procedure was used to generate ten model trees with different random sequences under equal boundary conditions of type PTP-F (see Table 1) within identical perfusion domains (rectangular slabs) and perfusion inlet position. Terminal flows were pre-set equal (conditions labeled PTP-constF in the following) so as to aim at a perfusion density as homogeneous as possible. Figure 1 (upper panels) shows two (of the ten) model realizations, clearly illustrating different gross anatomies due to the different random sequences. These structural differences represent the model correlate to anatomical variability among individuals as previously investigated (Schreiner *et al.*, 1997a). Despite different gross anatomies, all other model characteristics (e.g. the branching pattern, morphometric and functional indices) were found to be very similar among realizations.

Another ten model trees were generated under PTP-USS conditions, all of them identical to the PTP-constF series regarding perfusion domains,

TABLE 1
Physiologic model parameters used as boundary conditions

Parameter	Meaning	Value
N_{term}	Number of terminal segments	6000
Q_{perf}	Total perfusion flow	500 ml min^{-1}
V_{perf}	Total perfusion volume	100 cm^3
p_{perf}	Perfusion pressure	100 mmHg
r_{root}	Radius of root segment	2 mm
η	Viscosity of blood	3.6 cp (centi poise)
γ	Bifurcation exponent	3.0

Note: Parameter adaptation followed the lines of our previous work (Karch *et al.*, 2000a), except for the bifurcation exponent which was chosen to allow for uniform shear stress ($\gamma = 3$).

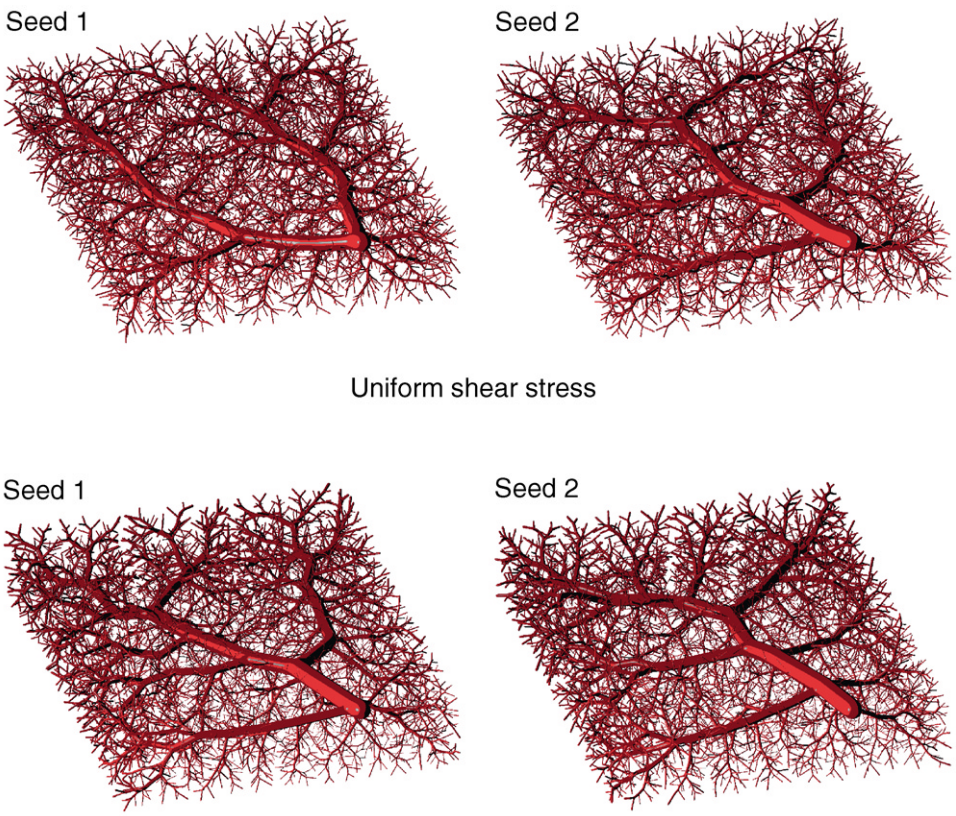

FIG. 1. 3D models generated by constrained constructive optimization. Upper panels: two realizations (with different seeds for the random number sequences) for boundary conditions with *pre-set terminal pressure and flows* (type PTP-constF). Lower panels: two realizations (using the same random number seeds as in upper panels) for boundary conditions with *pre-set terminal pressure and uniform shear stress* (type PTP-USS).

doi:10.1006 jtbi.2003.3136

inlet sites, perfusion pressure, root radius and total flow. Two of these realizations are shown in the lower panels of Fig. 1.

These two groups of trees were generated in order to allow for a direct comparison and separation of the effects induced by the constraints (PTP-constF vs. PTP-USS).

MORPHOLOGIC AND FUNCTIONAL DIFFERENCES INDUCED BY HOMOGENEOUS PERFUSION VERSUS UNIFORM SHEAR STRESS

Global Quantities

Global quantities assume one single value for a specific model tree: total volume, total surface, the sum of all segments' lengths, terminal pressure, the maximum Strahler order (Strahler, 1957), the maximum bifurcation order (Ley *et al.*, 1986), etc. The results are shown in Table 2.

The ten trees generated from different random seeds within each set of boundary conditions appeared very different in their "gross anatomies" (cf. Fig. 1), but very similar regarding global quantities. This confirms a previous finding: even trees with totally different routes of the large vessels may deviate by less than 1% in their global quantities, as long as boundary conditions and optimization targets are identical (Schreiner *et al.*, 1997a).

Switching to PTP-USS boundary conditions, however, obviously changes global quantities:

- Most obvious is the decline in (maximum) bifurcation order from an average of 59.5 to 49.2.
- The total intravascular volume—which is the optimization target in both cases—comes out larger (+4%), whereas the total endothelial surface declines (–7%).
- Terminal pressures and total segment length are affected by less than 1%.

Bifurcation Angles Compared with Experimental Values

Bifurcation angles in the model not only depend to the optimization target (Schreiner *et al.*, 1994) but also on the boundary conditions. This becomes evident in scatter plots of branching angle vs. symmetry index $\xi_{rad} = r_2/r_1$ (van Bavel & Spaan, 1992; Kamiya & Togawa, 1972; Zamir & Chee, 1986).

Experimental values for the angle θ_2 (i.e. the angle between parent and smaller daughter) vs. ξ_{rad} are shown in Fig. 2(A).

In the model results for PTP-constF conditions, shown in Fig. 2(B), most bifurcations seem to belong to a lengthy cluster. On top of that, a subgroup of bifurcations forms a conspicuous, arch-shaped cluster. Further investigation reveals that these data points represent that subclass of segments which feed exactly two terminals [$N_{dist} = 2$; marked with square symbols (□) in Fig. 2]. The surprising emergence of that cluster can be explained as follows: since all terminal flows have been set equal in the PTP-constF trees, l_2/l_1 (and thus the branching angle into sister terminals) uniquely depends on $\xi_{rad} = r_2/r_1$ due to eqn (6). Although this dependency

TABLE 2
Global quantities computed from CCO Trees

Quantity	Unit	COO mode		Difference	*P*
		PTP-const F	PTP-USS	(PTP-USS−PTP-const F)	
Total volume	(cm^3)	2.54±0.006	2.65±0.005	0.11	<0.0001*
Total surface	(cm^2)	181±0.25	168±0.20	−13.0	< 0.0001*
Total Σ length	(m)	18.4±0.02	18.5±0.02	0.1	< 0.0001*
p_{term}	(mmHg)	93.3±0.02	92.5±0.01	−0.8	< 0.0001*
Maximum Bifurcation order	(None)	59.5±2.9	49.2±1.8	−10.3	0.002†
Maximum Strahler order	(None)	6.9±0.3	6.9 ±0.3	0.0	1.0†

*Paired *t*-test.

†Wilcoxon matched-pairs signed-rank test.

For each mode (PTP-constF and PTP-USS) ten trees were generated. Values are given as mean±S.D. Differences due to boundary conditions were evaluated and tested for statistical significance.

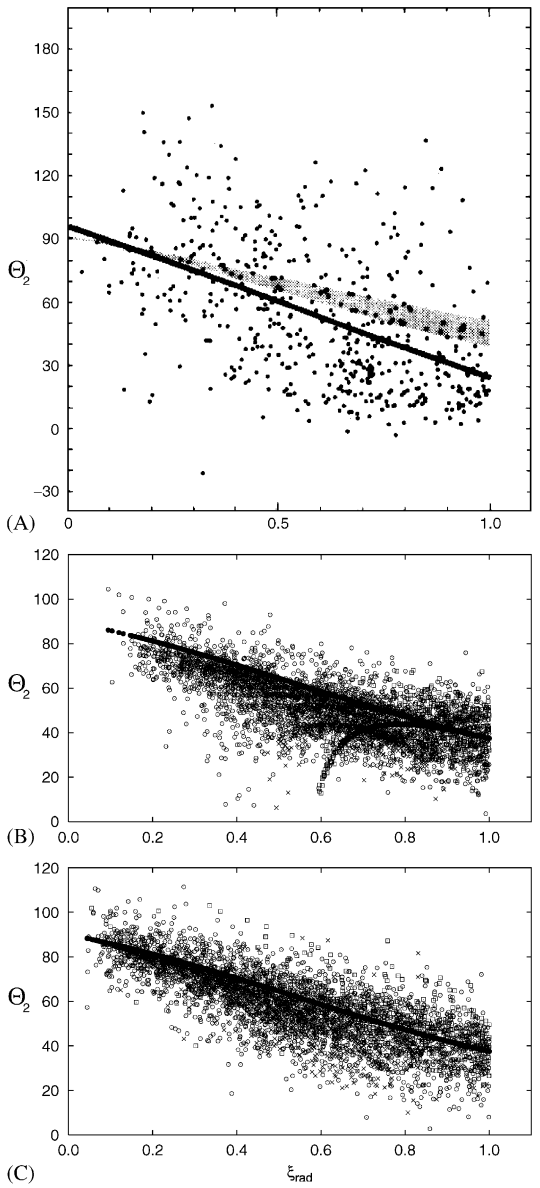

FIG. 2. Branching angles for different boundary conditions in comparison to experimental values. Vertical axes: branching angle (θ_2) between smaller daughter (radius r_2) and parent segment. Horizontal axes: symmetry index $\xi_{rad} = r_2/r_1$. (A) Bifurcation angles from experimental measurements, reproduced with kind permission from the work of Zamir (Zamir & Chee, 1986). The shaded region represents angles which are optimum on theoretical grounds, the broken line represents the linear regression to the data. (B) CCO model with pre-set equal terminal flows as boundary conditions (mode PTP-constF). These induce subclasses of segments, visible in arch-like clusters (see Discussion). (□) Bifurcations of segments supplying two terminals, (×) bifurcations of segments supplying more than two terminals. (C) CCO model with uniform shear stress (mode PTP-USS). The 'natural' dispersion in terminal flows induces a realistic distribution of branching angles. Symbols as in (B).

cannot be derived as an analytical formula (Kamiya & Togawa, 1972), it results from numerical geometric optimization.

Model trees under PTP-USS conditions obey Murray's law ($Q \propto r^3$) (Murray, 1926a, b), and a theoretical formula for optimum branching angles applies (Kamiya *et al.*, 1974; Kamiya & Togawa, 1972). Figure 2(C) shows the theoretical prediction (solid line) for θ_2 together with the model values, again grouped according to N_{dist} of the parent segment. Interestingly, there is no arc-shaped cluster to be seen, and all data rather gather around the theoretical prediction.

Conclusions from these findings will be addressed in the discussion.

DUAL RELATION BETWEEN THE VARIABILITIES IN SHEAR STRESS AND FLOW

Equal terminal flows represent a special choice of PTP-F conditions which inevitably induces variability in shear stress, even for $\gamma = 3$.

The proof is given indirectly from eqn (7): requiring equal flows ($Q_i = Q_i$) for a pair of sister terminals, equal shear stress is only possible if also the segments' lengths are equal ($l_i = l_j$). This is generally not the case, and one arrives at non-equal shear stresses even at the pre-terminal level if terminal flows are equal. This spread in pre-terminal shear stress propagates toward proximal and is found all over the tree, even for $\gamma = 3$. Note that $\gamma = 3$ is a necessary but not a sufficient condition for uniform shear stress in a binary tree.

On the contrary, for shear stress to be uniform, terminal flows must in general be different according to eqns (5) and (7).

We thus find something like a dual relation between the variability in terminal flows and the variability in shear stress: *shear stress can only be uniform at the expense of flow heterogeneity, and vice versa*. Figure 3 shows the resulting distributions of flow and shear stress in terminal segments:

(a) With equal terminal flows (represented by a point- or delta distribution of flow) we find a distribution of shear stress very close to

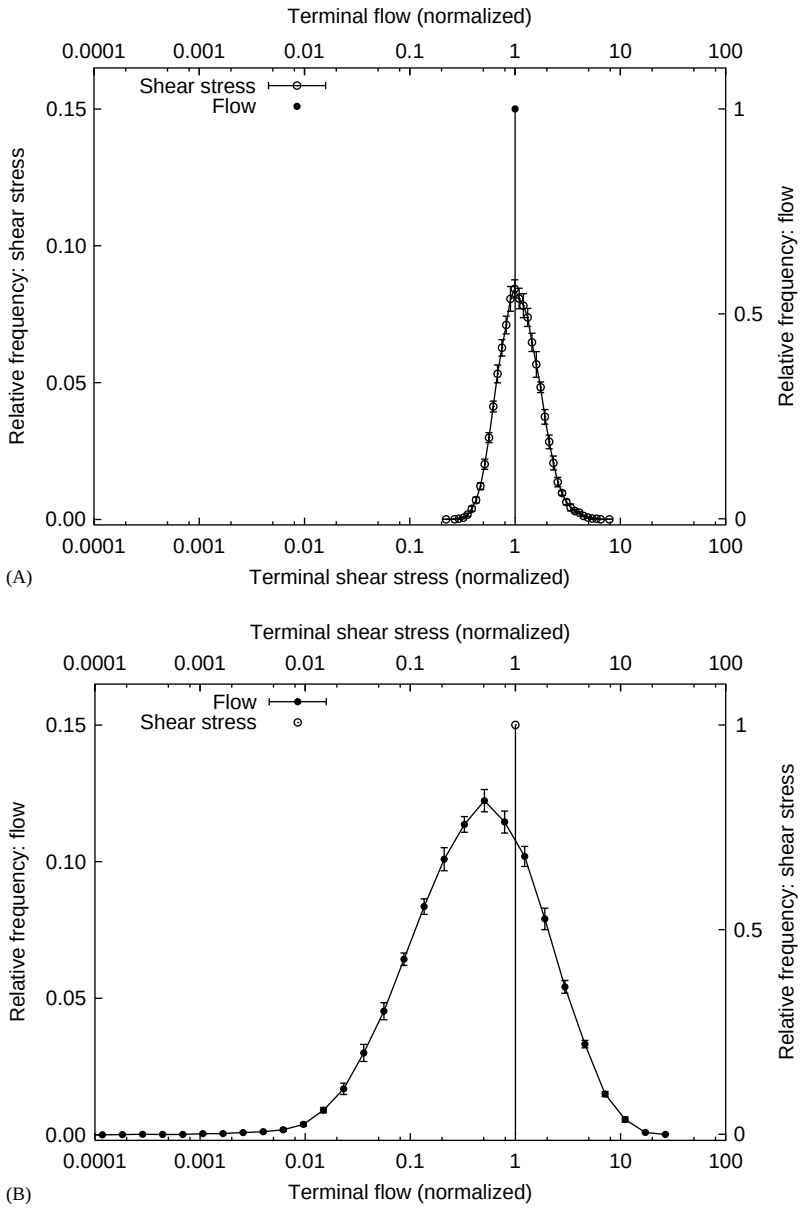

FIG. 3. Dual relation between dispersion of shear stress and dispersion of flow. (A) X-axis bottom: shear stress (normalized, i.e. divided by the value of shear stress in the root segment of each tree). *Y*-axis left: relative frequency of shear stress in terminal segments. Data are given as mean values (○), bars indicate standard deviations of frequencies, computed from ten trees generated under PTP-constF conditions with constant terminal flows. *X*-axis top: terminal flow (normalized, i.e. divided by the average terminal flow). *Y*-axis right: relative frequency of flow. Only one single value occurs [relative frequency = 1 (●)], corresponding to equal terminal flows. (B) *X*-axis bottom: terminal flow (normalized, i.e. divided by the average terminal flow). *Y*-axis left: relative frequency of flow in terminal segments. Data are given as mean values (●), bars indicate standard deviations of frequencies, computed from the ten realizations under uniform shear stress conditions (mode PTP-USS). X-axis top: terminal shear stress (normalized, i.e. divided by the shear stress in the root segment of each respective tree). *Y*-axis right: relative frequency of shear stress. Only one single value occurs [relative frequency = 1(○)], corresponding to uniform shear stress conditions.

log-normal [see Fig. (A)] with a relative dispersion (RD) of 0.48–0.50.

(b) Conversely, under uniform shear stress (i.e. with a point distribution in shear stress) we find a distribution of terminal flows looking close to log-normal [see Fig. 3(B)] with a relative dispersion (RD) of 1.5–1.6.

The magnitudes of dispersions and their relation to measurements will be evaluated in the final part of the ''Results'' section.

Model Fineness and Flow Heterogeneity

Model fineness is characterized by the number of terminals (N_{term}) in relation to the total perfusion volume (V_{perf}). For example, if a CCO tree with $N_{\text{term}} = 6000$ is grown into a perfusion volume of $100\,\text{cm}^3$, each terminal supplies on the average a "terminal" volume $\text{TV} = 100\,\text{cm}^3/6000 = 0.016\,\text{cm}^3$. Under PTP-F conditions we may choose equal terminal flows (PTP-constF) and thus obtain zero flow heterogeneity between TVs (for arguments please see the Discussion). Conversely, for PTP-USS conditions a "natural", log-normal flow distribution results among TVs. For $N_{\text{term}} = 6000$ we obtained $RD \approx 1.57$ for TVs of $0.016\,\text{cm}^3$. This value is somewhat larger than most experimental measurements (Bassingthwaighte *et al.*, 1985, 1989, 1994; Decking & Schrader, 1998; Pries *et al.*, 1996; Hoffman, 1995; Wolpers *et al.*, 1990; Wieringa *et al.*, 1982).

In order to scrutinize the source and magnitude of flow dispersion, additional CCO trees under uniform shear stress conditions were generated with $N_{\text{term}} = 50$, 100, 200, 500, 1000, 2000 and 4000. Even within this wide range of N_{term}, the increase in RDs of terminal flows (from 1.16 to 1.57, see Fig. 4) seems small, in particular when considering that in real arterial trees RDs decrease linearly (in a log–log plot) with increasing TV (Bassingthwaighte *et al.*, 1994).

Sources of Flow Heterogeneity Under Uniform Shear Stress Conditions

The terminal flows obtained under PTP-USS conditions were analysed in order to find out if there is some morphometric or structural quantity explaining a certain part of the RD observed. Among several candidates (e.g. "path-length from inlet", "bee-line-distance from inlet") the bifurcation level ($\Lambda :=$ number of bifurcations to traverse along the path from a segment toward the root of the tree) proved a key determinant [see Fig. 5(A)]: *under uniform shear stress conditions* (*PTP-USS*) *terminal flows increased markedly with bifurcation level*. In a log plot the dependency was fitted by a straight line

$$\log_{10}(Q_i^{USS}) = a + b\Lambda \tag{9}$$

with regression coefficients $a = -1.888$, $b = 0.0469$ and an $R^2 = 0.51$. [Throughout the present work "log()" is used for $\log_{10}()$].

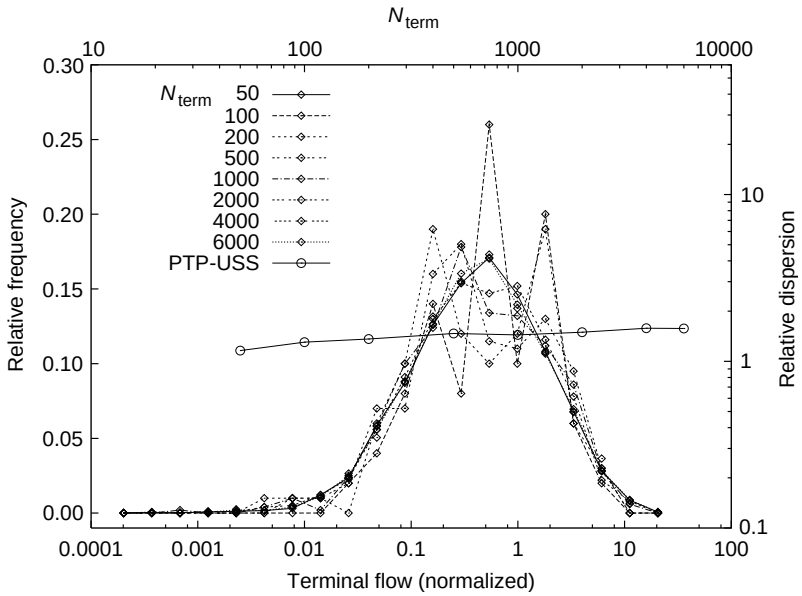

FIG. 4. Terminal flow distribution for different degrees of fineness of model trees. Vertical axis left: relative frequency. Horizontal axis bottom: terminal flow, normalized by its mean value $[Q_i/(Q_{\text{perf}}/N_{\text{term}})]$. Each of the bell-shaped curves represents a tree with a different N_{term}, see legend. All trees have been generated under PTP-USS conditions. Vertical axis right: relative dispersion of terminal flows. Horizontal axis top: N_{term}.

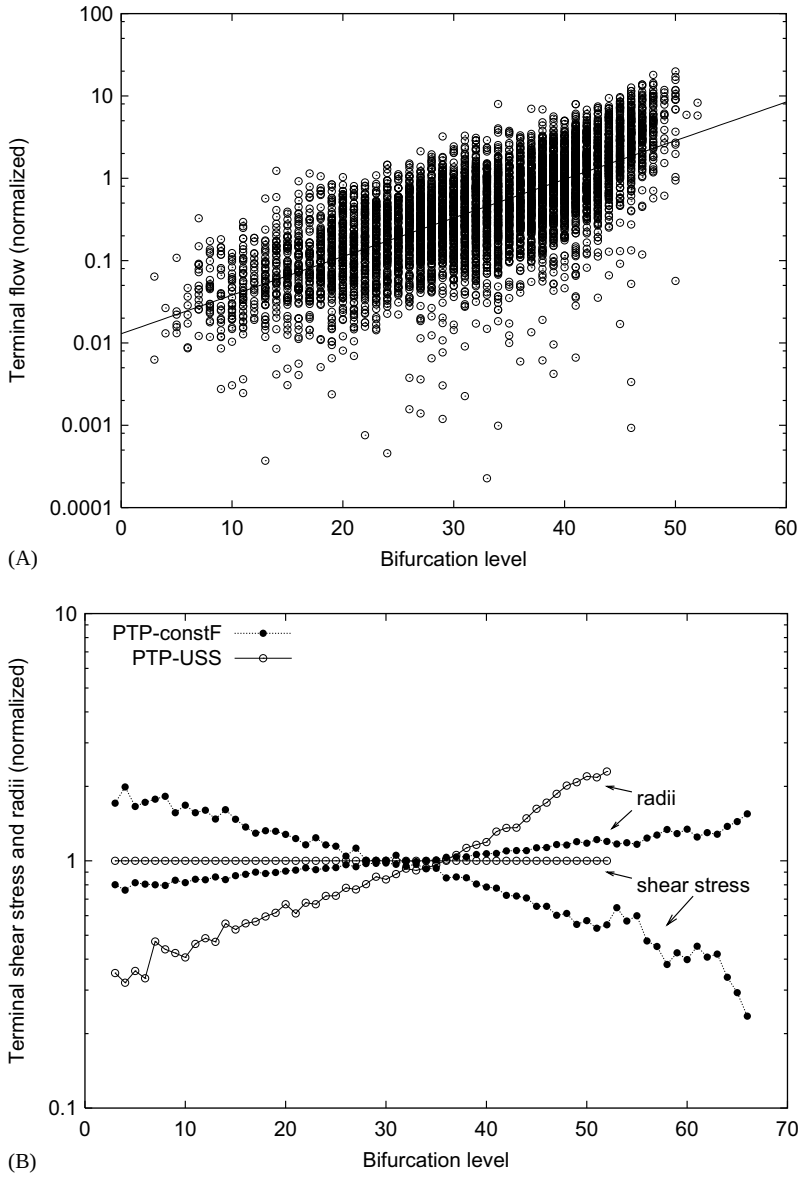

FIG. 5. Terminal flows under constF versus USS conditions. Horizontal axes: bifurcation level Λ. (●) PTP-constF (conditions with pre-set constant terminal flows). (○): PTP-USS (conditions with uniform shear stress). (A) Vertical axis: normalized terminal flows: $(Q_i/(Q_{\text{perf}}/N_{\text{term}})$. Note the systematic increase of terminal flows with bifurcation level as a consequence of uniform shear stress boundary conditions. See eqn (9) for the regression. (B) Vertical axis: normalized quantities (terminal shear stress and terminal radii, see arrows). Each symbol represents the average of the corresponding quantity within the bifurcation level.

Accordingly, 51% of the total dispersion of log flows are attributable to a linear increase with Λ, and the residual variability around the regression line has an average relative dispersion of 1.13.

The systematic increase in terminal flows, as represented by the regression line, amounts to a factor of approximately 200 when comparing terminals close to the inlet with terminals in the most remote parts of the tree (corresponding to the range $3 \leqslant \Lambda \leqslant 52$). The ambitious goal of implementing uniform shear stress turns out to induce most severe side effects regarding flow, which would deteriorate the model's physiological meaningfulness. No tissue whatsoever could tolerate differences in supply density by a factor of 200. Nevertheless, an "even" distribution of

shear stress remains a condition reasonable to aim at (Kassab & Fung, 1995).

Figure 5(B) shows the dependency of radii and shear stress on bifurcation level, contrasting PTP-constF with PTP-USS conditions. Under constF conditions (solid circles) terminal vessels widen slightly with increasing bifurcation level and shear stress declines drastically, almost by a factor of 10. Under USS conditions (open circles), terminal radii widen drastically with bifurcation level (about a factor of 6) in order to keep shear stress constant.

Discussion

SPECIFIC MODEL RESULTS AND COMPARISON WITH EXPERIMENTAL DATA

Boundary conditions of uniform shear stress (PTP-USS) entail several interesting aspects, in particular when compared to models generated with preset constant terminal flows (PTP-constF).

Bifurcation Angles

The bifurcation angles gather around the theoretical prediction curve in both cases, very similar to the experimental values (see Fig. 2). However, the artifact of an arch-shaped cluster seen under PTP-constF, caused by discrete values of flow in all terminal and pre-terminal segments, disappears under PTP-USS. This is a consequence of the more realistic (continuous) distribution of terminal and pre-terminal flows under PTP-USS conditions.

Bifurcation Levels and Asymmetry

Bifurcation symmetry (defined by the bifurcation index $\xi_{\text{rad}} = r_2/r_1$, van Bavel & Spaan, 1992) has often been related to the number of bifurcation levels occurring in a tree (Kassab *et al.*, 1993; van Beek *et al.*, 1989; Bassingthwaighte *et al.*, 1990; Schreiner *et al.*, 1997b; van Bavel & Spaan, 1992). In general, more asymmetric trees have a larger number of bifurcation levels ('conveying type of structure', Zamir, 1988b) down to their most distal terminals. Trees optimized under PTP-USS conditions need less bifurcation levels to split into a given number (N_{term}) of terminals than do PTP-constF trees, cf. Table 2. One might speculate that PTP-USS trees should therefore bifurcate more symmetrically. The opposite is true, however, when evaluating ξ_{rad} (results not shown). The puzzle is solved by the argument that bifurcation levels and symmetry are severely influenced by the flow distribution required at the terminals. In the case of PTP-USS, nothing is required regarding terminal flows and they come out very heterogeneous indeed. About 50 bifurcation levels suffice for that kind of distribution task. Imposing PTP-constF conditions, however, renders a much more "elaborate" task to solve, more levels are generated by optimization even though single bifurcations are more symmetric (larger ξ_{rad}) on the average.

The differences in structure are also reflected in the distribution of terminal segments over bifurcation levels (see Fig. 6, upper part).

Power Consumption for Perfusion

All model trees considered in the present work have been scaled to convey the same total perfusion flow and have the same radius at the inlet of the root segment, see Table 1. Another requirement was that all terminal pressures within each tree should be equal. p_{term} was computed so as to allow the desired perfusion flow. Therefore the power consumption (P) to overcome viscous resistance is given by

$$P = Q_{\text{perf}}(p_{\text{perf}} - p_{\text{term}}), \tag{10}$$

where Q_{perf} and p_{perf} are pre-set and constant, whereas p_{term} is computed. Among trees with different seeds but equal boundary conditions, p_{term} varies by less than one promille (Table 2), equivalent to a relative spread in power consumption of about $0.02/(100–93) \cong 0.00028$. This supports our previous hypothesis (Schreiner *et al.*, 1997a), namely that even trees with totally different gross anatomies (see Fig. 1) may show almost equal 'performances'.

The impact of boundary conditions on power consumption also is surprisingly small: between 1 and 2% in p_{term} (see Table 2), causing 11%

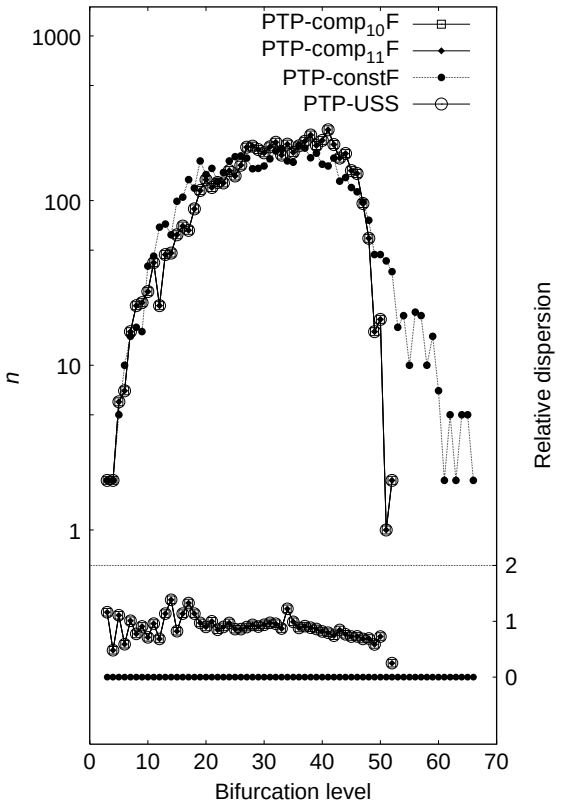

FIG. 6. Number of segments and relative flow dispersion within bifurcation levels. Left vertical axis (relevant for curves shown in upper part of graph): number of terminal segments (total for each tree: $N_{\text{term}} = 6000$). Right vertical axis (relevant for curves shown in lower part of graph): relative dispersion of terminal flows. (○) PTP-USS, (●) PTP-constF. Note that for PTP-constF (constant flows) $RD \equiv 0$ results (by definition) for each bifurcation level.

difference in power consumption between PTP-constF and PTP-USS, cf. eqn (10).

Flow Heterogeneity: *Features and Sources*

The main goal of the present work was to demonstrate that arterial tree models can be optimized for minimum intravascular volume under boundary conditions of uniform shear stress. The main results can be listed and explained as follows:

(a) Uniform shear stress induces heterogeneous terminal flows. Dispersions in flow and shear stress appear in a dual relation: eliminating the dispersion in terminal flows automatically induces a shear-stress dispersion and vice versa.

This finding becomes evident by considering the degrees of freedom in the system: specifying equal terminal flows (on top of total flow and radius of root segment, see Table 1) represents N_{term}–1 conditions imposed and thereby yields a unique solution for all hemodynamic quantities in the system. Shear stresses are computed quantities and come out heterogeneous in this case. If one requires equal terminal shear stresses instead, these N_{term}–1 conditions replace those for terminal flows, which then become computed quantities and result heterogeneous. Note that under a bifurcation law [eqn (1)] with $\gamma = 3$, equal terminal shear stresses will imply that all shear stresses are equal due to the continuity equation [eqn (3)], without any additional conditions being imposed.

The first component of flow heterogeneity under PTP-USS conditions is the "*local heterogeneity*", most directly to be seen between sister terminals, cf. eqn (7): flow is proportional to segment lengths cubed. The longer of two sister terminals has the massively larger flow. In terms of pressure gradient the relation is just inverse: the terminal with lower pressure gradient has larger flow.

The local nature of this mechanism is the same for all bifurcation levels, and suggests why relative dispersion of flow *within bifurcation levels* does not increase over bifurcation level, (see Fig. 6, lower part, open circles), even though average terminal flow increases massively with bifurcation level [Fig. 5(A)].

(b) Under uniform shear stress conditions, terminal flows show a systematic, massive (200%) increase toward large bifurcation orders and thus depend on a structural parameter.

This "*large-scale systematic flow heterogeneity*" within PTP-USS trees can be understood by extending the above argument to a whole path from the root to a terminal site: if shear stress is held constant, then flow is proportional to the third power of radius [due to eqn (6)] and radius is inversely proportional to pressure gradient $\Delta p_i/l_i$ due to

$$\frac{\Delta p_i}{l_i} = \frac{8\eta}{\pi} \underbrace{\frac{Q_i}{r_i^3}}_{\text{const.}} \frac{1}{r_i} \propto \frac{1}{r_i}. \tag{11}$$

Therefore flow is inversely proportional to the third power of pressure gradient. As a consequence, *long flow pathways* have (on the average over their length from root to terminal) lower pressure gradients and hence *must carry larger flows*.

(c) Increasing the fineness (i.e. increasing N_{term}) causes only a small increase in relative flow dispersion from 1.16 to 1.57 (Fig. 4).

While experimental measurements show a significant increase in relative dispersion of flows as the sample volume decreases (Bassingthwaighte *et al*., 1989; Iversen & Nicolaysen, 1995), the RD in the model does not. The reasons become evident by considering the above arguments regarding local and large-scale flow variabilities. Although increasing N_{term} will reduce the average length of terminals, it will not directly change the *ratios* in lengths between sister terminals [which induces heterogeneity, cf. eqn (7)]. Also the pathlength from root to any terminal somewhere within the perfusion area will not change massively as N_{term} increases. The average pressure gradients along paths to given locations will therefore remain rather constant and give rise to roughly the same ''large-scale flow variability'' depicted by the regression line in Fig. 5(A), almost regardless of N_{term}.

(d) Under uniform shear stress the distribution of terminal flows is close to log-normal.

This feature can be related to the central limit theorem (Papoulis, 1991; Qian & Bassingthwaighte, 2000): each terminal flow can be viewed as the product of multiple flow-split ratios,

$$Q_i = \prod_{\substack{j \in \{\text{path from } i \text{ to root}\} \\ k \text{ is parent of } j}} Q_j/Q_k. \qquad (12)$$

Provided that all paths had equal numbers of bifurcations and the flow ratios were independently drawn from some random distribution, their product would be approximately log-normally distributed. Each of these conditions is only partially fulfilled with PTP-USS conditions and one can only expect a mixture of distributions. As a matter of fact, however, the actual result quite closely resembles a log-normal one.

CONCEPTUAL ISSUES REVISITED: WHICH BOUNDARY CONDITIONS TO CHOOSE?

''A vascular tree should satisfy many physiological requirements from the organs and tissues conjugated at its terminals'' (Kamiya & Togawa, 1972). Within a model tree, these requirements have to be represented by appropriate boundary conditions. Among these, a uniform terminal pressure is commonly accepted as a reasonable choice (Kamiya & Togawa, 1972). However, due to limited computational resources, the fineness (N_{term}) of the present CCO models must remain far below that of real vascular beds. This is reflected in a small overall pressure difference around 8 mmHg (cf. Table 2) instead of about (100–40 =) 60 mmHg for real beds. The model thus does not yet reach the pre-capillary level at which constant pressure should prevail according to physiology. One possibility to bridge the 'pressure gap' would be to assume a constant resistance distal to each terminal, so as to have a black-box microcirculatory unit finally draining into a constant-pressure reservoir rather than the terminal segments themselves. This would be the option of choice to arrive at a model as realistic as possible with present resources, but it would introduce additional assumptions. For the present and more basic investigation, it was assumed that the model extends distally as far as a constant-pressure reservoir, knowing that the conceptual conclusions will be unaffected by the absolute magnitude of the pressure difference. It will be just a matter of increased computational speed in future technology to cope with N_{term} in the order of 10^6 and let p_{term} reach realistic values of pre-capillary pressure.

Another issue of debate is the distribution of flows to be supplied by the terminals. In the first version of CCO (Schreiner & Buxbaum, 1993), constant flows were assigned. In other models obtained from self-similar generators, terminal flows were prescribed by drawing random numbers from reasonable statistical distributions (Dawant *et al*., 1985; Levin *et al*., 1986; Popel *et al*., 1988), an approach which in the meantime has also become feasible for CCO models (Karch *et al*., 2000b). It allows to choose the underlying terminal flow distribution more or less deliberately, for example so as to ''exactly'' reproduce

experimental findings (Bassingthwaighte *et al.*, 1985, 1989; Deussen, 1998). If such an assignment is made during model growth, assigned flows will influence the developing structure. If the flow assignment is made *post hoc* (i.e. within a fully developed model), terminal flows need not relate to the arterial structure (segment locations, lengths, angles) proximal to an individual terminal and may result in a certain inconsistency between structure and flows in such models.

Another very interesting approach are fractal (self-similar) models in which not only structure (positions, lengths, angles) but also ratios of flows at bifurcations are prescribed by the generator (Beard & Bassingthwaighte, 2000; van Beek *et al.*, 1989; van Bavel & Spaan, 1992). In these models, flow splitting and structure may well be linked to each other, but need not be. Terminal flows result from multiple successive (prescribed) flow-split ratios rather than being finally imprinted. Not only is this concept capable of linking structure to individual flows, but it can even be shown on theoretical grounds that the resulting distribution of terminal flows approaches log-normality, regardless of the flow-split ratios chosen (Qian & Bassingthwaighte, 2000). The only drawback remaining in these models is that they do not guarantee spatial arrangeability of their segments: the real arterial systems—from which the probability distributions for lengths, radii, etc. are obtained—exist in space and fill a certain perfusion volume without intersecting segments. The model re-obtained through a self-similar generator—even if it is based on random numbers from these very distributions—does not automatically imply that the model will again be arrangeable in space.

In order to manage spatial arrangeability, growth models have been developed (Smith *et al.*, 2000; Van *et al.*, 1998; Schreiner, 1993; Karch *et al.*, 1997), among which the CCO approach derives vascular structures from optimization principles. An advantageous geometrical arrangement of segments and the space-filling property of terminals can be reached to a satisfying extent. However, up to now, terminal flows still had to be assigned somewhat deliberately: in early stages flows were set constant, later on drawn from random distributions (Karch *et al.*, 1997). Thus, also in these models a possible discrepancy between the (optimized) structure proximal to a terminal and the flow through this very terminal could not be ruled out. Moreover, our previous investigation (Schreiner *et al.*, 1999) revealed a very broad and unrealistic shear-stress distribution in CCO models with constant terminal flows. Hence in the present work, as a remedy, the distribution of shear stress should become a guiding factor of model generation, either as optimization target or as boundary condition.

Shear stress itself as an optimization target has been found inadequate by others (Hacking *et al.*, 1996) and ourselves, since it proved unstable during optimization (saddle point in the target function). As an alternative, *shear stress was incorporated in the boundary conditions* of the CCO algorithm. On the basis of well-established concepts (Murray & Oster, 1984; Zamir & Brown, 1982; Uylings, 1977; Zamir, 1976; Kamiya *et al.*, 1974; Murray, 1926a,b; Kamiya & Togawa, 1972; Sherman, 1981; Sherman *et al.*, 1989; Frame & Sarelius, 1995) the power law for radii [eqn (1)] was retained as a necessary but not sufficient condition. On top of that, the concepts outlined in the ''Methods'' section were implemented in order to prescribe flows giving rise to uniform shear stress allover the tree. However, disregarding any kind of mechanism toward uniform distribution of blood induced two types of flow heterogeneity (''local'' and ''large scale'') in which large flows massively favor long pathways and which is almost independent of model fineness.

On the basis of these results, several directions of future development shall be envisaged in the final section.

Critique of Generality of Conclusions

It may be argued that the relations between the variabilities in flow and shear stress have only been demonstrated for CCO models and might not be valid in general.

This is true in a quantitative but not in a conceptual sense for the following reasons: model trees generated by some other algorithm

(either another mode of CCO, a fractal generator, etc.) will yield quantitatively different RDs in flows when being scaled to uniform shear stress. However, the principal arguments leading to the very specific type of heterogeneity will remain valid, regardless of how in particular the model was generated.

Future Prospects

While the "mega-tree", with N_{term} in the order of 10^6, will most probably be an issue of speeding up algorithms, there are a lot of conceptual issues to be scrutinized in the future on the basis of CCO models. Three perspectives shall briefly be outlined.

Our latest findings about widespread shear stress as a consequence of equal terminal flows (Schreiner *et al.*, 1999) were the motivation for the present work: according to many suggestions from other scientists in the field we tried to homogenize shear stress by setting $\gamma = 3$ [eqn (1)]. After all $\gamma = 3$ is necessary for *totally uniform* shear stress (LaBarbera, 1990). However, looking at the consequences—the resulting terminal flow distribution—this "pure goal" of homogeneous shear stress seems questionable at least. Once we dismiss the goal of totally uniform shear stress and ask only for low spread in shear stress, it is no longer sure that $\gamma = 3$ remains the optimum choice. Perhaps some other value or even a variable γ—dependent on the position within the tree—might be more efficient in calming down shear stress heterogeneity while retaining some reasonable flow distribution. Several findings and arguments in the literature point in that direction (Woldenberg & Horsfield, 1983; Sherman, 1981; Roy & Woldenberg, 1982; Zamir *et al.*, 1992; van Bavel & Spaan, 1992; Kassab & Fung, 1995; Arts *et al.*, 1979; Kurz *et al.*, 1997; West *et al.*, 1997; Frame & Sarelius, 1995; Rossitti & Lofgren, 1993; Zamir & Brown, 1982; Zamir, 1988a). As perspective (i) CCO trees could be generated with variable or even adaptive γ ; its (parameterized) dependence on radius, Strahler order, bifurcation level, etc. could be optimized according to criterions involving both, dispersion of flow and shear stress in order to approach optimality. Any such approach would draw on a "bifurcation law" imposed on the system.

A conceptually different approach—perspective (ii)—draws on the argument that no mechanism in real arterial beds is known that could impose a given geometrical relationship between vessel diameters at bifurcations. Instead, the diameter of each branch is set by the individual vessels' structural responses to a number of stimuli, most notably wall shear stress and pressure (Pries *et al.*, 1998). Rather than plugging in a bifurcation law one would prescribe the adaptation mechanisms of individual segments (possible also including cooperative phenomena between adjacent vessels) and let the adaptation process yield radii. From these, something like a bifurcation law could be read off (e.g. a distribution of γ). This "law" would then no longer be understood as a governing concept but rather as a *post hoc* description of what had resulted from adaptation processes. A possible implementation of these mechanisms could either act on fully developed CCO trees, by adapting radii while leaving the connective structure, segment lengths and branching angles unchanged, or else—and computationally exceedingly more expensive—adaptation would occur concurrently with model development and optimization.

Perspective (iii) of future research is seen in the fractal properties of model trees. CCO models are an alternative approach to generate highly complex structures, from which distributions of fractal properties may be estimated rather than being plugged in. Since the CCO structures emerge from optimality principles in conjunction with boundary conditions, the relation between these and deduced fractal properties remains to be investigated.

The authors thank Alexandra Kaider, M. S., for valuable discussions regarding the statistical evaluations, and Mrs Claudia Holzer for preparing the manuscript. Special and explicit credit is given to an unknown reviewer for several essential points contributed to this work.

REFERENCES

Arts, T., Kruger, R. T. I., van Gerven, W., Lambregts, J. A. C. & Reneman, R. S. (1979). Propagation

velocity and reflection of pressure waves in the canine coronary artery. *Am. J. Physiol.* **237,** H469–H474.

Bassingthwaighte, J. B., King, R. B., Hales, J. R. S. & Rowell, L. B. (1985). Stability of heterogeneity of myocardial blood flow in normal awake baboons. *Cir. Res.* **57,** 285–295.

Bassingthwaighte, J. B., King, R. B. & Roger, S. A. (1989). Fractal nature of regional myocardial blood flow heterogeneity. *Cir. Res.* **65,** 578–590.

Bassingthwaighte, J. B., Liebovitch, L. S. & West, B. J. (1994). *Fractal Physiology*, pp. 1–364. New York: Oxford University Press.

Bassingthwaighte, J. B., van Beek, J. H. & King, R. B. (1990). Fractal branchings: the basis of myocardial flow heterogeneities? *Ann. N. Y. Acad. Sci.* **591,** 392–401.

Beard, D. A. & Bassingthwaighte, J. B. (2000). The fractal nature of myocardial blood flow emerges from a whole-organ model of arterial network. *J. Vasc. Res.* **37,** 282–296.

Brown, M. D. & Egginton, S. (1988). Capillary density and fine structure in rabbit papillary muscles after a high dose of norepinephrine. *Microvasc. Res.* **36,** 1–12.

Caro, C. G., Parker, K. H. & Doorly, D. J. (1995). Essentials of blood flow. *Perfusion* **10,** 131–134.

Cohn, D. L. (1954). Optimal systems: I. The vascular system. *Bull. Math. Biophys.* **16,** 59–74.

Davies, P. F., Dewey, C. F. Jr., Bussolari, S. R., Gordon, E. J. & Gimbrone, M. A. Jr. (1984). Influence of hemodynamic forces on vascular endothelial function. *In vitro* studies of shear stress and pinocytosis in bovine aortic cells. *J. Clin. Invest.* **73,** 1121–1129.

Dawant, B., Levin, M. & Popel, A. S. (1985). Effect of dispersion of vessel diameters and lengths in stochastic networks I. Modeling of microcirculatory flow. *Microvasc. Res.* **31,** 203–222.

Decking, U. K. & Schrader, J. (1998). Spatial heterogeneity of myocardial perfusion and metabolism. *Basic Res. Cardiol.* **93,** 439–445.

Deussen, A. (1998). Blood flow heterogeneity in the heart. *Basic Res. Cardiol.* **93,** 430–438.

Frame, M. D. & Sarelius, I. H. (1995). Energy optimization and bifurcation angles in the microcirculation. *Microvasc. Res.* **50,** 301–310.

Franke, R. P., Gräfe, M., Schnittler, H., Seiffge, D. & Mittermayer, C. (1984). Induction of human vascular endothelial stress fibres by fluid shear stress. *Nature* **307,** 648–649.

Fröberg, C. E. (1985). *Numerical mathematics. Theory and Computer Applications,* pp. 184–186. Menlo Park, CA, U.S.A.: Benjamin/Cummings.

Fung, Y. C. (1997). *Biomechanics. Circulation.* New York: Springer-Verlag.

Gimbrone-MA. J. (1999). Endothelial dysfunction, hemodynamic forces, and atherosclerosis. *Thromb. Haemost.* **82,** 722–726.

Girard, P. R. & Nerem, R. M. (1995). Shear stress modulates endothelial cell morphology and F-actin organization through the regulation of focal adhesion-associated proteins. *J. Cell. Physiol.* **163,** 179–193.

Hacking, W. J., vanBavel, E. & Spaan, J. A. (1996). Shear stress is not sufficient to control growth of vascular networks: a model study. *Am. J Physiol.* **270,** H364–H375.

Hazel, A. L. & Pedley, T. J. (2000). Vascular endothelial cells minimize the total force on their nuclei. *Biophys. J.* **78,** 47–54.

Hellums, J. D. & Hardwick, R. A. (1981). Response to platelets to shear stress — a review. In: *Hemovascular Rheology: the Physics of Blood and Vascular Tissue* (Hwang, N. H. C. & Gross, D. R., eds), pp. 160–183. Amsterdam: Sijthoff and Noorhoff.

Hoffman, J. I. (1995). Heterogeneity of myocardial blood flow. *Basic Res. Cardiol.* **90,** 103–111.

Iversen, P. O. & Nicolaysen, G. (1995). Fractals describe blood flow heterogeneity within skeletal muscle and within myocardium. *Am. J. Physiol.* **268,** H112–H116.

Jones, C. J. H., Kuo, L., Davis, M. J. & Chilian, W. M. (1993). Myogenic and flow-dependent control mechanisms in the coronary microcirculation [editorial]. *Basic Res. Cardiol.* **88,** 2–10.

Kamiya, A. & Togawa, T. (1972). Optimal branching structure of the vascular tree. *Bull. Math. Biophys.* **34,** 431–438.

Kamiya, A., Togawa, T. & Yamamoto, A. (1974). Theoretical relationship between the optimal models of the vascular tree. *Bull. Math. Biol.* **36,** 311–323.

Karch, R., Schreiner, W., Neumann, F. & Neumann, M. (1997). Three-dimensional optimization of arterial tree models. In: *Simulation in Biomedicine.* (Power, H., Brebbia, C. A. & Kenny, J. eds), Vol. IV pp. 3–12. Southampton: Computational Mechanics Publications.

Karch, R., Neumann, F., Neumann, M. & Schreiner, W. (1999). A three-dimensional model for arterial tree representation, generated by constrained constructive optimization. *Comput. Biol. Med.* **29,** 19–38.

Karch, R., Neumann, F., Neumann, M. & Schreiner, W. (2000a). Staged growth of optimized arterial model trees. *Ann. Biomed. Eng.* **28,** 495–511.

Karch, R., Schreiner, W., Neumann, F. & Neumann, M. (2000b). Modeling of coronary vascular trees: generating optimized structures. In: *Medical Applications of Computer Modelling: Cardiovascular and Ocular Systems* (Martonen, T. B. ed.), pp. 59–74. Southampton, Boston: WIT Press.

Kassab, G. S. & Fung, Y. C. (1995). The pattern of coronary arteriolar bifurcations and the uniform shear hypothesis. *Ann. Biomed. Eng.* **23,** 13–20.

Kassab, G. S., Rider, C. A., Tang, N. J. & Fung, Y.-C. B. (1993). Morphometry of pig coronary arterial trees. *Am. J. Physiol.* **265,** 350–365.

Knuth, D. (1973). *The Art of Computer Programming. Vol.1: Fundamental Algorithms.* Reading, MA: Addison-Wesley.

Kurz, H., Sandau, K. & Christ, B. (1997). On the bifurcation of blood vessels—Wilhelm Roux's doctoral thesis (Jena 1878)—a seminal work for biophysical modelling in developmental biology. *Anat. Anz.* **179,** 33–36.

LaBarbera, M. (1990). Principles of design of fluid transport systems in zoology. *Science* **249,** 992–999.

Lefevre, J. (1982). Teleonomical representation of the pulmonary arterial bed of the dog by a fractal tree. In: *Cardiovascular System Dynamics: Models and Measurements* (Kenner, T. Busse R. & Hinghofer-Szalkay, H. eds.), pp. 137–146. New York, London: Plenum Press.

Lefevre, J. (1983). Teleonomical optimization of a fractal model of the pulmonary arterial bed. *J. theor. Biol.* **102,** 225–248.

Leverett, L. D., Hellums, J. D., Alfrey, C. P. & Lynch, E. C. (1972). Red blood cell damage by shear stress. *Biophys. J.* **12,** 157–173.

Levin, M., Dawant, B. & Popel, A. S. (1986). Effect of dispersion of vessel diameters and lengths in stochastic networks II. Modeling of microvascular hematocrit distribution. *Microvasc. Res.* **31,** 223–34.

Ley, K., Pries, A. R. & Gaehtgens, P. (1986). Topological structure of rat mesenteric microvessel networks. *Microvasc. Res.* **32,** 315–332.

Murray, C. D. (1926a). The physiological principle of minimum work. I. The vascular system and the cost of blood volume. *Proc. Natl. Acad. Sci. U.S.A.* **12,** 207–214.

Murray, C. D. (1926b). The physiological principle of minimum work applied to the angle of branching of arteries. *J. Gen. Physiol.* **9,** 835–841.

Murray, J. D. & Oster, G. F. (1984). Generation of biological pattern and form. *IMA J. Math. Appl. Med. Biol.* **1,** 51–75.

Papoulis, A. (1991). *Probability, Random Variables and Stochastic Processes*, pp. 1–666. New York: McGraw-Hill.

Popel, A. S., Liu, A., Dawant, B., Koller, A. & Johnson, P. C. (1988). Distribution of vascular resistance in terminal arteriolar networks of cat sartorius muscle. *Am. J. Physiol*. **254,** H1149–H1156.

Pries, A. R., Secomb, T. W., Gaehtgens, P. & Gross, J. F. (1990). Blood flow in microvascular networks. Experiments and simulation. *Cir. Res.* **67,** 826–834.

Pries, A. R., Secomb, T. W. & Gaehtgens, P. (1995). Design principles of vascular beds. *Cir. Res.* **77,** 1017–1023.

Pries, A. R., Secomb, T. W. & Gaehtgens, P. (1996). Relationship between structural and hemodynamic heterogeneity in microvascular networks. *Am. J. Physiol.* **270,** H545–H553.

Pries, A. R., Secomb, T. W. & Gaehtgens, P. (1998). Structural adaptation and stability of microvascular networks: theory and simulations. *Am. J. Physiol.* **275,** H349–H360

Qian, H. & Bassingthwaighte, J. B. (2000). A class of flow bifurcation models with lognormal distribution and fractal dispersion. *J. theor. Biol.* **205,** 261–268.

Rodbard, S. (1975). Vascular caliber. *Cardiology.* **60,** 4–49.

Rosen, R. (1967). *Optimality Principles in Biology.* London: Butterworth & Co. Ltd.

Rossitti, S. & Lofgren, J. (1993). Vascular dimensions of the cerebral arteries follow the principle of minimum work. *Stroke* **24,** 371–377.

Roy, A. G. & Woldenberg, M. J. (1982). A generalization of the optimal models of arterial branching. *Bull. Math Biol.* **44,** 349–360.

Schreiner, W. (1993). Computer generation of complex arterial tree models. *J. Biomed. Eng.* **15,** 148–150.

Schreiner, W. & Buxbaum, P. F. (1993). Computer-optimization of vascular trees. *IEEE Trans. Biomed. Eng.* **40,** 482–491.

Schreiner, W., Neumann, M., Neumann, F., Roedler, S. M., End, A., Buxbaum, P. F., Müller, M. R. & Spieckermann, P. (1994). The branching angles in computer-generated optimized models of arterial trees. *J. Gen. Physiol.* **103,** 975–989.

Schreiner, W., Neumann, F., Neumann, M., End, A., Roedler, S. M. & Aharinejad, S. (1995). The influence of optimization target selection on the structure of arterial tree models generated by constrained constructive optimization. *J. Gen. Physiol.* **106,** 583–599.

Schreiner, W., Neumann, M., Neumann, F. & Karch, R. (1996). Constrained constructive optimization: Methode und Ergebnisse. *Biomed. Tech.* 41 Suppl. **1,** 124–125.

Schreiner, W., Neumann, F., Neumann, M., End, A. & Roedler, S. M. (1997a). Anatomical variability and functional ability of vascular trees modeled by constrained constructive optimization. *J. theor. Bio.* **187,** 147–158.

Schreiner, W., Neumann, F., Neumann, M., Karch, R., End, A. & Roedler, S. M. (1997b). Limited bifurcation asymmetry in coronary arterial tree models generated by constrained constructive optimization. *J. Gen. Physiol.* **109,** 129–140.

Schreiner, W., Neumann, F., Karch, R., Neumann, M., Roedler, S. M. & End, A. (1999). Shear stress distribution in arterial tree models, generated by constrained constructive optimization. *J. theor. Biol.* **198,** 27–45.

Schubothe, M., Vetterlein, F. & Schmidt, G. (1983). Density of plasma-perfused capillaries in the rat heart during carbocromene-induced vasodilation. *Basic Res. Cardiol.* **78,** 113–123.

Sherman, T. F. (1981). On connecting large vessels to small: the meaning of MURRAY's law. *J. Gen. Physiol.* **78,** 431–453.

Sherman, T. F., Popel, A. S., Koller, A. & Johnson, P. C. (1989). The cost of departure from optimal radii in microvascular networks. *J. theor. Biol.* **136,** 245–265.

Skalak, T. C. & Price, R. J. (1996). The role of mechanical stresses in microvascular remodeling. *Microcirculation* **3,** 143–165.

Smith, N. P., Pullan, A. J. & Hunter, P. J. (2000). Generation of an anatomically based geometric coronary model. *Ann. Biomed. Eng.* **28,** 14–25.

Strahler, A. N. (1957). Quantitative analysis of watershed geomorphology. *Trans. Am. Geophys. Union* **38,** 913–920.

Thompson, D. W. (1942). *On Growth and Form.* Cambridge: Cambridge University Press.

Topper, J. N. & Gimbrone-MA. J. (1999). Blood flow and vascular gene expression: fluid shear stress as a modulator of endothelial phenotype. *Mol. Med. Today* **5,** 40–46.

Uylings, H. B. M. (1977). Optimization of diameters and bifurcation angles in lung and vascular tree structures. *Bull. Math. Biol.* **39,** 509–519.

van Bavel, E. & Spaan, J. A. E. (1992). Branching patterns in the porcine coronary arterial tree. Estimation of flow heterogeneity. *Cir. Res.* **71,** 1200–1212.

van Beek, J. H. G. M., Roger, S. A. & Bassingthwaighte, J. B. (1989). Regional myocardial flow heterogeneity explained with fractal networks. *Am. J. Physiol.* **257,** H1670–H1680

van, L. G., Kotte, A. N. & Lagendijk, J. J. (1998). A flexible algorithm for construction of 3-D vessel networks

for use in thermal modeling. *IEEE Trans. Biomed. Eng.* **45,** 596–604.

West, G. B., Brown, J. H. & Enquist, B. J. (1997). A general model for the origin of allometric scaling laws in biology. *Science* **276,** 122–126.

Wieringa, P. A., Spaan, J. A. E., Stassen, H. G. & Laird, J. D. (1982). Heterogeneous flow distribution in a three dimensional network simulation of the myocardial microcirculation—a hypothesis. *Microcirculation* **2,** 195–216.

Woldenberg, M. J. & Horsfield, K. (1983). Finding the optimal lengths for three branches at a junction. *J. theor. Biol.* **104,** 301–318.

Wolpers, H. G., Hoeft, A., Korb, H., Lichtlen, P. R. & Hellige, G. (1990). Heterogeneity of myocardial blood flow under normal conditions and its dependence on arterial PO2. *Am. J. Physiol.* **258,** 549–555.

Yung, W. & Frojmovic, M. M. (1982). Platelet aggregation in laminar flow. Adenosine diphosphate concentration, time and shear rate dependence. *Thromb. Res.* **28,** 361–377.

Zamir, M. (1976). Optimality principles in arterial branching. *J. theor. Biol.* **62,** 227–251.

Zamir, M. (1988a). The branching structure of arterial trees. *Comments theor. Biol.* **1,** 15–37.

Zamir, M. (1988b). Distributing and delivering vessels of the human heart. *J. Gen. Physiol.* **91,** 725–735.

Zamir, M. & Bigelow, D. C. (1984). Cost of deparature from optimality in arterial branching. *J. theor. Biol.* **109,** 401–409.

Zamir, M. & Brown, N. (1982). Arterial branching in various parts of the cardiovascular system. *Am. J. Anat.* **163,** 295–307.

Zamir, M. & Chee, H. (1986). Branching characteristics of human coronary arteries. *Can. J. Physiol. Pharmacol.* **64,** 661–668.

Zamir, M., Sinclair, P. & Wonnacott, T. H. (1992). Relation between diameter and flow in major branches of the arch of the aorta. *J. Biomech.* **25,** 1303–1310.

Zhou, Y., Kassab, G. S. & Molloi, S. (1999). On the design of the coronary arterial tree: a generalization of Murray's law. *Phys. Med. Biol.* **44,** 2929–2945.